

Metrological performance of a single-channel brain-computer interface based on motor imagery

*Original*

Metrological performance of a single-channel brain-computer interface based on motor imagery / Angrisani, L.; Arpaia, P.; Donnarumma, F.; Esposito, A.; Moccaldi, N.; Parvis, M.. - ELETTRONICO. - 2019-:(2019), pp. 1-5. (Intervento presentato al convegno 2019 IEEE International Instrumentation and Measurement Technology Conference, I2MTC 2019 tenutosi a Auckland, New Zeland nel 2019) [10.1109/I2MTC.2019.8827168].

*Availability:*

This version is available at: 11583/2848086 since: 2020-10-10T15:29:34Z

*Publisher:*

IEEE

*Published*

DOI:10.1109/I2MTC.2019.8827168

*Terms of use:*

This article is made available under terms and conditions as specified in the corresponding bibliographic description in the repository

*Publisher copyright*

IEEE postprint/Author's Accepted Manuscript

©2019 IEEE. Personal use of this material is permitted. Permission from IEEE must be obtained for all other uses, in any current or future media, including reprinting/republishing this material for advertising or promotional purposes, creating new collecting works, for resale or lists, or reuse of any copyrighted component of this work in other works.

(Article begins on next page)

# Metrological performance of a single-channel Brain-Computer Interface based on Motor Imagery

Leopoldo Angrisani<sup>1</sup>, Pasquale Arpaia<sup>1</sup>, Francesco Donnarumma<sup>2</sup>,  
Antonio Esposito<sup>3</sup>, Nicola Moccaldi<sup>1</sup>, and Marco Parvis<sup>3</sup>

**Abstract**—In this paper, the accuracy in classifying Motor Imagery (MI) tasks for a Brain-Computer Interface (BCI) is analyzed. Electroencephalographic (EEG) signals were taken into account, notably by employing one channel per time. Four classes were to distinguish, i.e. imagining the movement of left hand, right hand, feet, or tongue. The dataset "2a" of BCI Competition IV (2008) was considered. Brain signals were processed by applying a short-time Fourier transform, a common spatial pattern filter for feature extraction, and a support vector machine for classification. With this work, the aim is to give a contribution to the development of wearable MI-based BCIs by relying on single channel EEG.

**Index Terms**—brain-computer interfaces, motor imagery, feature extraction, classification accuracy.

## I. INTRODUCTION

Brain-computer interfaces (BCI) have been studied extensively since their first proposal in 1973 [1]. The interest in these technologies has exploded in the last 20 years, and BCIs have become a rapidly growing research area [2]. A BCI measures the brain activity trying to understand the user's intention through a specific feature of the acquired signal. The extracted feature is classified, and then translated into a command for a computer or other devices. This way of communication with the external world does not depend on the brain's normal output pathways, namely peripheral nerves and muscles [3]. For this reason, it has been mainly studied for people with motor disabilities and rehabilitation purposes [4]–[6]. However, recent trends foresee their employment in fields like gaming [7] or robotics [8].

Many paradigms have been proposed for BCIs. Many rely on visually-evoked potentials (VEP), which usually require little training and have good performance [9]–[12]. However, these paradigms also require external stimulation. Instead, a BCI based on Motor Imagery (MI) does not depend upon external stimulation, but they suffer of inter-subject variability, require long training, and performance are not as good as in the case of VEPs [13], [14]. Non-invasive measurements techniques are here taken into account. Among these, the mostly used is electroencephalography (EEG), which measures the electrical activity of neurons with electrodes placed on the user's scalp [15]. The focus is on single-channel EEG for a highly wearable and portable device.

Several studies focused on EEG channel selection for classifying motor imagery signals [14], [16]–[18], showing that the minimum channels number can span from 5 up to 20 or more. The number of channels could also depend on the subject. Most works on Motor Imagery considered two imagery tasks, usually imagining left hand movement versus right hand movement [19], [20]. The two classes are then mapped on more commands aiming to control an external device, such as a wheelchair or a robot. Sometimes, hybrid approaches are employed to increase the number of possible commands [21], [22]. Fewer studies considered a BCI with four motor imagery tasks. For instance, in [23], a control interface is proposed for driving a car in a virtual environment considering four MI tasks: imagining left hand movement, right hand movement, both hands, or both feet.

The first work on a single-channel BCI and four motor imagery tasks was conducted by Sheng Ge et al. in 2014 [24]. As better discussed later, they propose to extract information from a single-channel EEG using a short-time Fourier transform, and then apply a common spatial pattern to filter signals and extract features for classification. They report a mean classification accuracy equal to 65% when employing the dataset IIIa from the 2005 BCI competition. The maximum accuracy they obtained was about 88%, and the input signals they could analyze were recorded for 4 s. This performance is to compare with other MI-based BCIs, employing multiple EEG channels or even hybrid approaches, where the classification accuracies span from 62% to 87% and, usually, the time windows are 1.00 s to 7.00 s wide.

The literature reports no other study combining single-channel and four tasks MI-based BCI after 2014, not even from the group of Mr. Ge [25]. In this paper, the aim is to improve the results of [24] starting from replicating the algorithm of Sheng Ge et al. with some modifications, while considering the dataset "2a" of BCI Competition IV (2008) [26]. A single channel among the available 22 EEG channels is selected, and the classification has to discriminate between four classes of signals recorded for 3 s. This work gives a contribution in the direction of building a highly wearable, low-cost, and easy-to-use BCI capable of interpreting four different motor imagery tasks. In the following, Section II recalls the signal processing reported in [24] and proposes some improvements, while Section III discusses the results obtained processing data extracted from the aforementioned dataset.

<sup>1</sup>Department of Electrical Engineering and Information Technology (DI-ETI), Università degli Studi di Napoli Federico II, Naples, Italy

<sup>2</sup>Institute of Cognitive Sciences and Technologies (ISTC), Consiglio Nazionale delle Ricerche, Rome, Italy

<sup>3</sup>Department of Electronics and Telecommunications (DET), Politecnico di Torino, Turin, Italy

## II. PROPOSED METHOD

### A. Data description

The dataset "2a" of 2008 BCI Competition IV is here considered. The data consist of signals from 9 subjects. The four different motor imagery tasks are the imagination of movement of the left hand (class 1), right hand (class 2), both feet (class 3), and tongue (class 4). For each subject, two sessions were recorded, training (T) and evaluation (E). Each session is comprised of 6 runs separated by short breaks. One run consists of 48 trials (12 runs per class), yielding a total of 288 trials per session. The 6 runs are preceded by 3 runs in which signals related to eye movements were recorded. These runs are not considered in this work. In each run of concern, data from 22 EEG channels and 3 EOG (electrooculography) channels are present. Only one EEG channel per time is considered and the 3 s related to the motor imagery task are extracted. Relying on the results of [24], only the channels C3, Cz, and C4 were taken into account. The channels name is consistent with the international 10-20 system [27]. More details on the experimental setup and the dataset itself are reported in [26]. In the following, the signal processing implemented in Matlab is reported. As already mentioned in the introduction, based the work is based on the processing proposed by Sheng Ge et al. aiming to improve it.

### B. Feature extraction

The signals extracted from the dataset were considered together with their class label and some other information given with the dataset, such as the sampling frequency of the EEGs. The labels were used during the first phase for training a classifier, and in the second phase to assess its classification accuracy. Fig. 1 reports the average signals obtained considering the trials of a single run separated per class (12 signals for each class). It is clear that the classes are not easy to discriminate in the time domain.

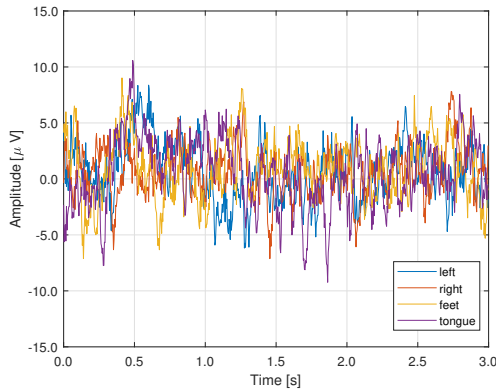


Fig. 1. Average brain signals corresponding to four motor imagery tasks.

According to [24], the signal is transformed in the frequency domain. In particular, by employing the short-time Fourier Transform (STFT), one can obtain the short-term, time-localized frequency content of each signal, thus aiming to

extract more information from a single EEG channel. Next, a Common Spatial Pattern (CSP) filter is adopted to obtain the principal components of the transformed data. Finally, features are extracted for classification. A Support Vector Machine (SVM) is exploited first. The three steps preceding classification are better described in the following.

1) *Short-time Fourier Transform*: exploiting the "spectrogram" function of Matlab, the short-time Fourier Transform was computed for each signal. A Hamming windowing was employed considering 100 samples for each time-instant. This window was zero-padded to 128 samples before calculating the frequency content. Consecutive windows had a 50% overlap. Considering the module of the spectrum, a real matrix  $X_j$  was associated to each brain signal. Thanks to the labels associated to the brain signals, the matrices can be separated per class. An example of spectrogram is reported in 2, where the mean of the matrices  $X_{j,4}$  associated to the class 4 ("tongue") was calculated.

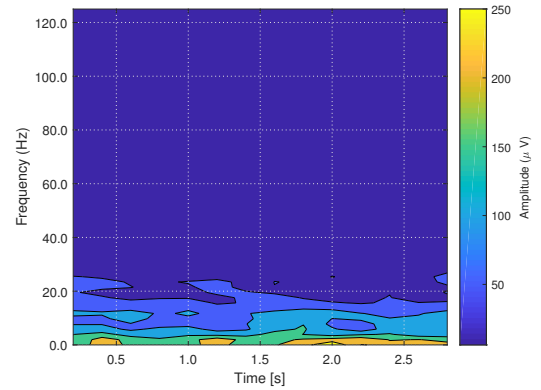


Fig. 2. Average spectrogram obtained considering the class "tongue".

2) *Common Spatial Pattern*: a CSP filter is usually employed to separate two different classes. With a binary CSP one can transform two classes of data into a common space, such that the two classes of transformed data have the same principal components, and their corresponding eigenvalues add up to a unit matrix. The transformation (or projection) matrices are found from training data. In the case of four classes, four projection matrices are found for four binary CSP. Each binary CSP separates one class from the rest (one versus the rest, OVR). The OVR algorithm follows the derivation of [24]. For each real matrix  $X_j$ , the covariance is calculated as

$$R_j = X_j X_j^T, \quad (1)$$

where  $X_j^T$  is the transposed matrix of  $X_j$ . Four covariance matrices,  $C_1$ ,  $C_2$ ,  $C_3$ , and  $C_4$ , are obtained as the mean of the covariance matrices separated per class. A composite covariance matrices is then

$$C = C_1 + C_2 + C_3 + C_4. \quad (2)$$

Diagonalization is applied to obtain  $U_0$  and  $\Lambda$  such that

$$C = U_0 \Lambda U_0^{-1}, \quad (3)$$

where  $U_0^{-1} = U_0^T$  because the covariance matrix is symmetric and real. A whitening transformation is also applied, and the chosen whitening matrix is

$$P = \Lambda^{-1/2} U_0^T \quad (4)$$

It is easy to demonstrate that this whitening matrix satisfies the condition  $P^T P = C^{-1}$ . The matrix  $P$  is thus obtained considering all classes. Instead, for each class  $i = 1, 2, 3, 4$  the matrices  $S_i$  are derived as

$$S_i = P C_i P^T \quad (5)$$

It can be demonstrated that  $S_i$  shares common principal components with

$$S'_i = P C'_i P^T = P \left( \sum_{k \neq i} C_k \right) P^T, \quad (6)$$

which is a matrix associated to the complementary of  $C_i$  (OVR). Hence,  $S_i$  and  $S'_i$  can be diagonalized with the same eigenvectors matrix  $U_i$ , and the sum of the respective diagonal matrices will be the unit matrix. The final projection matrices are found as

$$W_i = U_i^T P \quad (7)$$

3) *Features calculation*: each spectrogram matrix  $X_j$  is projected into four new matrices associated to four classes,

$$Z_{j,i} = W_i X_j, \quad (8)$$

and features are extracted prior to classification with an SVM. The matrix  $W_i$  (in the present case its dimension is  $65 \times 65$ ), can be "cut" considering the first  $m$  rows and the last  $m$  rows. This is done aiming to consider the principal components. An example of projected spectrogram is depicted in Fig. 3, where  $m = 4$  was set.

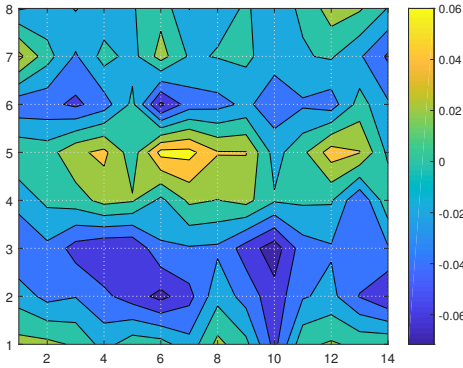


Fig. 3. Spectrogram associated to the average between the signals of class "tongue" after projection with the CSP filter ( $m = 4$ ).

As suggested in [24], features that can be considered are

$$f_i = \log \frac{\sigma_i^2}{\sum_{i=1}^4 \sigma_i^2} \quad i = 1, 2, 3, 4 \quad (9)$$

where  $\sigma_i^2$  is the variance of  $Z_i$  among time points. Hence, for each trial, there are  $4 \cdot 2m$  signal features useful for classification.

### C. Classification

The signal features classification is here conducted with a Support Vector Machine (SVM) [28]. The idea of SVM is to find a hyperplane that best separates the data points of different classes while maximizing the margin, even though errors are allowed during separation. The input to be classified is mapped to a high-dimensional feature space with a "kernel function". Aiming to classify signals belonging to four classes, the Matlab function *fitcecoc* is employed. It fits multi-class models, and hence it fulfills the need of the present case study. A  $8m \times n_{tr}$  feature matrix is passed to the function together with the  $1 \times n_{tr}$  array of labels.  $n_{tr}$  is the number of considered trials. Usually, a "gaussian kernel" is suggested for the analysis of non-stationary signals like EEG signals. However, simulations showed that a "linear kernel" leads to greater accuracies in the considered case.

The classifier was cross-validated with a 10-fold procedure. This means that 10 iterations were conducted, and, in each iteration, the 90% of the dataset was considered for training, while the remaining 10% was considered for validation. The procedure is done applying the Matlab function *crossval* to the previously found SVM model. The classification accuracy was calculated with the function *kfoldLoss*, applied to the cross-validated SVM. This Matlab function gives back the percentage of classification loss (misclassification). Hence, to evaluate the accuracy accuracy of learned feature weights on test data, one can consider

$$accuracy = 1 - loss. \quad (10)$$

## III. RESULTS

The signal processing algorithm described in the previous section was implemented in Matlab. The extraction of signals from the datasets, the application of a common spatial pattern, and the features calculations were conducted with functions implemented ad hoc. Though data from 9 subjects are available in the BCI Competition IV dataset "2a", only 3 subjects are considered, i.e. "A01T", "A02T", and "A05T". For each subject, the all 6 runs were considered, thus implying that 288 trials ( $6 \cdot 48$ ) were available for the cross-validation procedure. Finally, the analysis was conducted on three EEG channels, C3, CZ, and C4. These are associated to the sensorimotor cerebral cortex. It is to remark that, aiming to study a single-channel BCI, one channel per time is considered.

In the following, the classification accuracies for each subject are plot as a function of the factor  $m$  defining the CSP filter dimension, and for the three different EEG channels. Fig. 4 shows the classification accuracies for the subject A01, notably considering the dataset portion "A01T". It can be seen that the accuracy grows up with  $m$ . This trend is also present for subjects A02 and A05 (Fig. 5 and 6).

It is to remark that there is and inter-subject variability. For instance, the accuracies achieved with the data "A01T" shown in Fig. 4 go up to the 90% and more, while the accuracies for "A02T" in Fig. 5 do not reach the 80%.

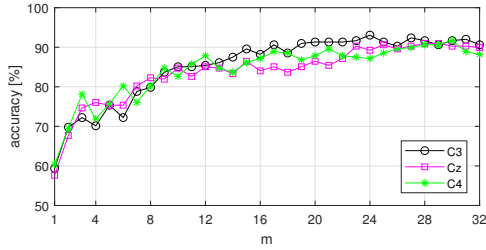


Fig. 4. Classification accuracy with the data "A01T" and three different EEG channels. A 10-fold cross validation procedure is here considered

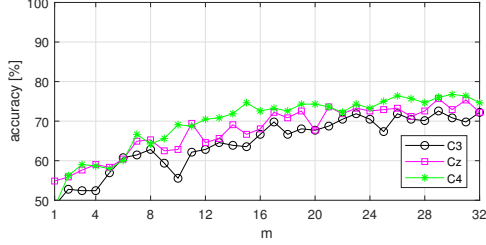


Fig. 5. Classification accuracy with the data "A02T" and three different EEG channels. A 10-fold cross validation procedure is here considered

Meanwhile, the results achieved for "A05T", shown in Fig. 6 are similar to the results of the subject A01. It is to remark that the values of accuracy are to refer to the 25%, that is the accuracy of a random classifier in the case of 4 classes. However, the minimum accuracy on the "y-axis" of the figures was set at 50% because this can be considered as a minimum acceptable value.

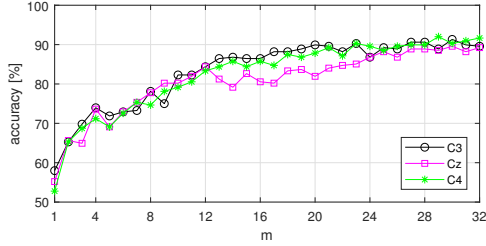


Fig. 6. Classification accuracy with the data "A05T" and three different EEG channels. A 10-fold cross validation procedure is here considered

Finally, the cross-validation procedure was repeated considering a 50-fold procedure, i.e. the 50% of data are used for training, and the validation is conducted on the remaining 50%. This is done to balance the amount of training data with the amount of validation one. The results are compatible with the results from the 10-fold cross-validation procedure. This aimed to show a robustness of the adopted cross-validation procedure.

Comparing the achieved results with the ones of [24], it is underlined that the values of accuracy seem compatible with those results as long as the  $m \leq 10$ . In addition, values of  $m$  up to 32 were also explored, which is the maximum

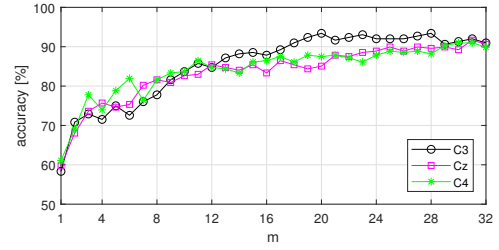


Fig. 7. Classification accuracy with the data "A01T" and three different EEG channels. A 50-fold cross validation procedure is here considered

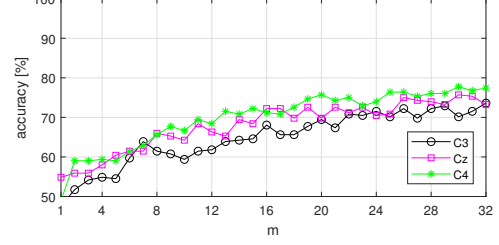


Fig. 8. Classification accuracy with the data "A02T" and three different EEG channels. A 50-fold cross validation procedure is here considered

possible (the  $W_i$  before cutting has dimension  $65 \times 65$ ). The classification results better when considering more filter components, in contrast with the results of [24], where the optimum was identified as  $m = 7$ . These results could indicate a reproducibility problem. Indeed, the data considered in this work were acquired with a different experimental setup if compared to the data of BCI Competition III considered by Sheng Ge et al. Future steps will thus be the analysis of data from BCI Competition III with the algorithm improvement discussed in this paper, thus providing a better comparison with the results of [24], and then the aim is to employ the SVM model characterized as described in this work, for the analysis of data from different subjects.

#### IV. CONCLUSIONS

This paper contributes to the study of motor imagery based brain computer interfaces (BCIs), by relying in particular on a single channel electroencephalography. Such a BCI system would guarantee high wearability, low cost, and easy use. However, the main limitation of a single channel device is the reduced amount of information, resulting in a difficulty to recognize the user's intention. The scope of the present study was to evaluate the accuracy of classification when 4 tasks have to be discriminated, namely imagining the movement of left hand, right hand, feet, or tongue.

A previous work by the group of Sheng Ge et al. was considered. It was conducted in 2014 and the dataset from the BCI Competition III was taken into account. Instead, the dataset "2a" of BCI Competition IV was here considered and some modifications were made to the signal processing, especially in the classification part. For the analysis of classification performance, the percentage of misclassified observations in



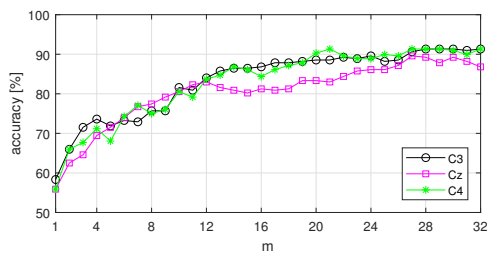


Fig. 9. Classification accuracy with the data "A05T" and three different EEG channels. A 50-fold cross validation procedure is here considered

a 10-fold cross-validation procedure is considered. This classification loss was translated into classification accuracy. It was shown that this accuracy is compatible with the results from the group of Mr. Ge, and that it can be improved if the parameter  $m$  of the CSP filter is increased. Following steps will be to apply the trained and cross-validated model to data from other BCI sessions. This aims to give a contribution to a very interesting BCI branch that has not been considered enough after 2014.

#### REFERENCES

- [1] J. J. Vidal, "Toward direct brain-computer communication," *Annual review of Biophysics and Bioengineering*, vol. 2, no. 1, pp. 157–180, 1973.
- [2] K. Hu, C. Chen, Q. Meng, Z. Williams, and W. Xu, "Scientific profile of brain-computer interfaces: Bibliometric analysis in a 10-year period," *Neuroscience letters*, vol. 635, pp. 61–66, 2016.
- [3] J. R. Wolpaw, N. Birbaumer, D. J. McFarland, G. Pfurtscheller, and T. M. Vaughan, "Brain-computer interfaces for communication and control," *Clinical neurophysiology*, vol. 113, no. 6, pp. 767–791, 2002.
- [4] J. R. Wolpaw, N. Birbaumer, W. J. Heetderks, D. J. McFarland, P. H. Peckham, G. Schalk, E. Donchin, L. A. Quatrano, C. J. Robinson, and T. M. Vaughan, "Brain-computer interface technology: a review of the first international meeting," *IEEE transactions on rehabilitation engineering*, vol. 8, no. 2, pp. 164–173, 2000.
- [5] R. Ortner, B. Z. Allison, G. Korisek, H. Gaggl, and G. Pfurtscheller, "An SSVEP BCI to control a hand orthosis for persons with tetraplegia," *IEEE Transactions on Neural Systems and Rehabilitation Engineering*, vol. 19, no. 1, pp. 1–5, 2011.
- [6] S. R. Soekadar, N. Birbaumer, M. W. Slutzky, and L. G. Cohen, "Brain-machine interfaces in neurorehabilitation of stroke," *Neurobiology of disease*, vol. 83, pp. 172–179, 2015.
- [7] D. Marshall, D. Coyle, S. Wilson, and M. Callaghan, "Games, gameplay, and bci: the state of the art," *IEEE Transactions on Computational Intelligence and AI in Games*, vol. 5, no. 2, pp. 82–99, 2013.
- [8] L. Bi, X.-A. Fan, and Y. Liu, "EEG-based brain-controlled mobile robots: a survey," *IEEE transactions on human-machine systems*, vol. 43, no. 2, pp. 161–176, 2013.
- [9] M. Cheng, X. Gao, S. Gao, and D. Xu, "Design and implementation of a brain-computer interface with high transfer rates," *IEEE transactions on biomedical engineering*, vol. 49, no. 10, pp. 1181–1186, 2002.
- [10] C. Guger, S. Daban, E. Sellers, C. Holzner, G. Krausz, R. Carabalona, F. Gramatica, and G. Edlinger, "How many people are able to control a P300-based brain-computer interface (BCI)?" *Neuroscience letters*, vol. 462, no. 1, pp. 94–98, 2009.
- [11] Y. Wang, R. Wang, X. Gao, B. Hong, and S. Gao, "A practical VEP-based brain-computer interface," *IEEE Transactions on Neural Systems and Rehabilitation Engineering*, vol. 14, no. 2, pp. 234–240, 2006.
- [12] S. Ajami, A. Mahnam, and V. Abootalebi, "Development of a practical high frequency brain-computer interface based on steady-state visual evoked potentials using a single channel of EEG," *Biocybernetics and Biomedical Engineering*, vol. 38, no. 1, pp. 106–114, 2018.
- [13] M. Ahn and S. C. Jun, "Performance variation in motor imagery brain-computer interface: a brief review," *Journal of neuroscience methods*, vol. 243, pp. 103–110, 2015.
- [14] C.-C. Lo, T.-Y. Chien, Y.-C. Chen, S.-H. Tsai, W.-C. Fang, and B.-S. Lin, "A wearable channel selection-based brain-computer interface for motor imagery detection," *Sensors*, vol. 16, no. 2, p. 213, 2016.
- [15] M. Teplan *et al.*, "Fundamentals of EEG measurement," *Measurement science review*, vol. 2, no. 2, pp. 1–11, 2002.
- [16] L. He, Y. Hu, Y. Li, and D. Li, "Channel selection by Rayleigh coefficient maximization based genetic algorithm for classifying single-trial motor imagery EEG," *Neurocomputing*, vol. 121, pp. 423–433, 2013.
- [17] H. Shan, H. Xu, S. Zhu, and B. He, "A novel channel selection method for optimal classification in different motor imagery BCI paradigms," *Biomedical engineering online*, vol. 14, no. 1, p. 93, 2015.
- [18] J. Long, Y. Li, and Z. Gu, "Channel selection for motor imagery-based BCIs: a semi-supervised SVM algorithm," in *Advances in Cognitive Neurodynamics (II)*, pp. 701–705, Springer, 2011.
- [19] M. Aljalal, R. Djemal, and S. Ibrahim, "Robot Navigation Using a Brain Computer Interface Based on Motor Imagery," *Journal of Medical and Biological Engineering*, pp. 1–15, 2018.
- [20] Y. Liu, W. Su, Z. Li, G. Shi, X. Chu, Y. Kang, and W. Shang, "Motor Imagery Based Teleoperation of a Dual-arm Robot Performing Manipulation Tasks," *IEEE Transactions on Cognitive and Developmental Systems*, 2018.
- [21] Y. Yu, Z. Zhou, Y. Liu, J. Jiang, E. Yin, N. Zhang, Z. Wang, Y. Liu, X. Wu, and D. Hu, "Self-paced operation of a wheelchair based on a hybrid brain-computer interface combining motor imagery and P300 potential," *IEEE Transactions on Neural Systems and Rehabilitation Engineering*, vol. 25, no. 12, pp. 2516–2526, 2017.
- [22] T. Ma, H. Li, L. Deng, H. Yang, X. Lv, P. Li, F. Li, R. Zhang, T. Liu, D. Yao, *et al.*, "The hybrid BCI system for movement control by combining motor imagery and moving onset visual evoked potential," *Journal of neural engineering*, vol. 14, no. 2, p. 026015, 2017.
- [23] H. Wang, T. Li, A. Bezerianos, H. Huang, Y. He, and P. Chen, "The control of a virtual automatic car based on multiple patterns of motor imagery BCI," *Medical & biological engineering & computing*, pp. 1–11, 2018.
- [24] S. Ge, R. Wang, and D. Yu, "Classification of four-class motor imagery employing single-channel electroencephalography," *PloS one*, vol. 9, no. 6, p. e98019, 2014.
- [25] S. Ge, Q. Yang, R. Wang, P. Lin, J. Gao, Y. Leng, Y. Yang, and H. Wang, "A brain-computer interface based on a few-channel eeg-fnirs bimodal system," *IEEE Access*, vol. 5, pp. 208–218, 2017.
- [26] C. Brunner, R. Leeb, G. R. Muller-Putz, A. Schlogl, and G. Pfurtscheller, "BCI competition 2008 Graz data set A," [http://www.bbci.de/competition/iv/desc\\_2a.pdf](http://www.bbci.de/competition/iv/desc_2a.pdf), 2008.
- [27] G. H. Klem, H. O. Lüders, H. Jasper, C. Elger, *et al.*, "The ten-twenty electrode system of the international federation," *Electroencephalogr Clin Neurophysiol*, vol. 52, no. 3, pp. 3–6, 1999.
- [28] C.-W. Hsu, C.-C. Chang, C.-J. Lin, *et al.*, "A practical guide to support vector classification," 2003.